would suffice to perform quantum simulations of multidimensional fermionic systems such as the Hubbard model that have proved resistant to conventional computational techniques. Hundreds to thousands of bits may be required to simulate accurately systems with continuous variables such as lattice gauge theories or models of quantum gravity. Current quantum logic devices can perform operations on two quantum bits (*23*, *24*, *26*); however, ion-trap quantum computers with a few tens of quantum bits apparently require only minor modifications of current technology (*24*). Although a quantum simulator with three or four quantum bits would be too small to solve classically intractable problems, it would still be large enough to test many of the ideas presented here. As suggested in (*13*), such simulators would also be able to create and test the properties of exotic quantum states such as Greenberger-Horne-Zeilinger states. Another possibility (*13*) is that by modulating the interactions between spins, atoms, or quantum dots in large arrays (*41*), one could perform massively parallel quantum simulations involving many quantum systems at once. The wide variety of atomic, molecular, and semiconductor quantum devices available suggests that quantum simulation may soon be a reality.

REFERENCES AND NOTES

1. P. Benioff, *J. Stat. Phys.* **22**, 563 (1980); *Phys. Rev. Lett.* **48**, 1581 (1982); *J. Stat. Phys.* **29**, 515 (1982); *Ann. N.Y. Acad. Sci.* **480**, 475 (1986).
2. R. P. Feynman, *Opt. News* **11**, 11 (1985); *Found. Phys.* **16**, 507 (1986); *Int. J. Theor. Phys.* **21**, 467 (1982).
3. W. H. Zurek, *Phys. Rev. Lett.* **53**, 391 (1984).
4. A. Peres, *Phys. Rev. A* **32**, 3266 (1985).
5. N. Margolus, *Ann. N.Y. Acad. Sci.* **480**, 487 (1986); in *Complexity, Entropy, and the Physics of Information*, vol. 8 of *Santa Fe Institute Series*, W. H. Zurek, Ed. (Addison-Wesley, Redwood City, CA, 1991), pp. 273–288.
6. D. Deutsch, *Proc. R. Soc. London Ser. A* **400**, 97 (1985).
7. See, however, D. Deutsch and R. Jozsa, *ibid.* **439**, 553 (1992), for an interesting oracle problem that can be performed more quickly by quantum computers.
8. D. Deutsch, *ibid.* **425**, 73 (1989).
9. Y. Yamamoto, M. Kitegawa, K. Igeta, in *Proceedings of the 3rd Asia-Pacific Physics Conference*, Y. W. Chan, A. F. Lenng, C. N. Yang, K. Young, Eds. (World Scientific, Singapore, 1988), pp. 779–799.
10. G. J. Milburn, *Phys. Rev. Lett.* **62**, 2124 (1989).
11. R. Landauer, *Int. J. Theor. Phys.* **21**, 283 (1982); *Found. Phys.* **16**, 551 (1986); *Nature* **335**, 779 (1988); in *Nanostructure Physics and Fabrication*, M. A. Reed and W. P. Kirk, Eds. (Academic Press, Boston, 1989), pp. 17–29; *Phys. Today* **42**, 119 (October 1989); in *Proceedings of the 3rd International Symposium on Foundations of Quantum Mechanics*, Tokyo, 28 to 31 August 1989 (Physical Society of Japan, Tokyo, 1990), p. 407; *Physica A* **168**, 75 (1990); *Phys. Today* **44**, 23 (May 1991); in *Proceedings of the Workshop on Physics of Computation II*, Dallas, 17 to 20 November 1994, D. Matzke, Ed. (IEEE Computer Society, Los Alamitos, CA, 1994), pp. 54–58.
12. K. Obermayer, W. G. Teich, G. Mahler, *Phys. Rev. B* **37**, 8096 (1988); W. G. Teich, K. Obermayer, G. Mahler, *ibid.*, p. 8111; W. G. Teich and G. Mahler, *Phys. Rev. A* **45**, 3300 (1992).
13. S. Lloyd, *Science* **261**, 1569 (1993); *ibid.* **263**, 695 (1994).
14. P. Shor, in *Proceedings of the 35th Annual Symposium on Foundations of Computer Science*, Santa Fe, NM, 20 to 22 November 1994, S. Goldwasser, Ed. (IEEE Computer Society, Los Alamitos, CA, 1994), p. 124.
15. D. P. DiVincenzo, *Science* **270**, 255 (1995).
16. ———, *Phys. Rev. A* **50**, 1015 (1995).
17. A. Barenco, D. Deutsch, A. Ekert, R. Jozsa, *Phys. Rev. Lett.* **74**, 4083 (1995).
18. T. Sleator and H. Weinfurter, *ibid.*, p. 4087.
19. G. M. Palma, K.-A. Suominem, A. Ekert, *Proc. R. Soc. London Ser. A* **452**, 567 (1996).
20. S. Lloyd, *Phys. Rev. Lett.* **75**, 346 (1995).
21. D. Deutsch, A. Barenco, A. Ekert, *Proc. R. Soc. London Ser. A* **449**, 669 (1995).
22. J. I. Cirac and P. Zoller, *Phys. Rev. Lett.* **74**, 4091 (1995).
23. Q. A. Turchette, C. J. Hood, W. Lange, H. Mabuchi, H. J. Kimble, *ibid.* **75**, 4710 (1995).
24. C. Monroe, D. M. Meekhof, B. E. King, W. M. Itano, D. J. Wineland, *ibid.*, p. 4714.
25. W. G. Unruh, *Phys. Rev. A* **51**, 992 (1995).
26. M. Brune *et al.*, *Phys. Rev. Lett.* **72**, 3339 (1994); P. Domokos, J. M. Raimond, M. Brune, S. Haroche, *Phys. Rev. A* **52**, 3554 (1995).
27. R. Landauer, *Philos. Trans. R. Soc. London Ser. A* **353**, 367 (1995); in *Proceedings of the Drexel-4 Symposium on Quantum Nonintegrability: Quantum Classical Correspondence*, D. H. Feng and B. L. Hu, Eds. (International Press, Boston, 1996).
28. I. L. Chuang, R. Laflamme, P. W. Shor, W. H. Zurek, *Science* **270**, 1633 (1995).
29. P. W. Shor, *Phys. Rev. A* **52**, 2493 (1995); A. R. Calderbank and P. W. Shor, *Phys. Rev. A*, in press; A. Steane, in preparation.
30. M. H. Kalos, Ed., *Monte Carlo Methods in Quantum Problems* (Reidel, Dordrecht, Netherlands, 1984).
31. K. Binder, Ed., *The Monte Carlo Method in Condensed Matter Physics* (Springer-Verlag, New York, 1995).
32. C. Rebbi, Ed., *Lattice Gauge Theories and Monte Carlo Simulations* (World Scientific, Singapore, 1983).
33. W. S. Warren, D. P. Weitekamp, A. Pines, *J. Chem. Phys.* **73**, 2084 (1980).
34. V. Ramakrishna, M. V. Salapaka, M. Dahleh, H. Rabitz, A. Peirce, *Phys. Rev. A* **51**, 960 (1995).
35. A. Yao, in *Proceedings of the 34th Annual Symposium on Foundations of Computer Science*, S. Goldwasser, Ed. (IEEE Computer Society, Los Alamitos, CA, 1995), p. 352.
36. H. Mabuchi and H. J. Kimble, *Opt. Lett.* **19**, 749 (1993); A. B. Matsko, S. P. Vyatchanin, H. Mabuchi, H. J. Kimble, *Phys. Lett. A* **192**, 175 (1994); H. J. Kimble *et al.*, in *Proceedings of the International Conference on Atomic Physics*; A. S. Parkins, P. Marte, P. Zoller, H. J. Kimble, *Phys. Rev. Lett.* **71**, 3095 (1993).
37. For the simulated trajectory always to remain within ε of the desired trajectory, the experimenter must be able to enact not only $e^{iH_j t}$, but $e^{-iH_j t}$ as well. See, for example, R. W. Brockett, R. S. Millman, H. J. Sussman, Eds., *Differential Geometric Control Theory* (Birkhauser, Boston, 1983), and Z. Li and J. F. Canney, Eds., *Nonholonomic Motion Planning* (Kluwer Academic, Boston, 1993).
38. The extra factor of N is required to conform with the normal rules for phases of fermions on a lattice in second quantized form. See, for example, A. L. Fetter and J. D. Walecka, *Quantum Theory of Many-Particle Systems* (McGraw-Hill, New York, 1971), and J. W. Negele and H. Ormand, *Quantum Many-Particle Systems* (Addison-Wesley, Redwood City, CA, 1988).
39. K. Kraus, *States, Effects, and Operations: Fundamental Notions of Quantum Theory* (Springer-Verlag, Berlin, 1983).
40. There is an extra subtlety in the open system case. For the quantum analog simulation of open systems to be efficient, the time evolution of the open system must be a finite-order quantum Markov process, that is, the environment must have finite time and space correlation lengths.
41. C. B. Murray, C. R. Kagan, M. G. Bawendi, *Science* **270**, 1335 (1995).

42. Supported in part by grant N00014-95-1-0975 from the Office of Naval Research. This work is part of the Quantum Information and Computation project (QUIC).

8 February 1996; accepted 10 June 1996

A Crosslinked Cofactor in Lysyl Oxidase: Redox Function for Amino Acid Side Chains

Sophie Xuefei Wang, Minae Mure,* Katalin F. Medzihradszky, Alma L. Burlingame, Doreen E. Brown, David M. Dooley, Alan J. Smith, Herbert M. Kagan, Judith P. Klinman†

A previously unknown redox cofactor has been identified in the active site of lysyl oxidase from the bovine aorta. Edman sequencing, mass spectrometry, ultraviolet-visible spectra, and resonance Raman studies showed that this cofactor is a quinone. Its structure is derived from the crosslinking of the ε-amino group of a peptidyl lysine with the modified side chain of a tyrosyl residue, and it has been designated lysine tyrosylquinone. This quinone appears to be the only example of a mammalian cofactor formed from the crosslinking of two amino acid side chains. This discovery expands the range of known quino-cofactor structures and has implications for the mechanism of their biogenesis.

Lysyl oxidase (LO, E.C. 1.4.3.13) is an extracellular, matrix-embedded protein. It has a central role in the biogenesis of connective tissue by way of posttranslational oxidative modification of the ε-amino group of lysine side chains in elastin and collagen to form inter- and intrachain crosslinks (*1*, *2*). The physiologic importance of LO is well established. Decreased LO activity is observed in diseases of im-

paired copper metabolism, as found in the human type IX Ehlers-Danlos syndrome and Menkes' syndrome, both of which are chromosome X–linked, recessively inherited disorders. Increased LO activity is associated with some fibrotic disorders such as atherosclerosis, hypertension, and liver and pulmonary disease. An understanding of the biogenesis, structure, and mechanism of LO should aid in the development of chemotherapeutic agents for the control of fibrotic diseases (*3*).

LO is considered a member of the copper amine oxidase (CAO) family because of its requirement for protein-bound copper and the nature of the reaction it catalyzes. CAOs catalyze the oxidative deamination of amines to aldehydes, concomitant with the reduction of dioxygen to hydrogen peroxide and the release of ammonia (Eq. 1):

$$RCH_2NH_2 + O_2 + H_2O \rightarrow RCHO + NH_3 + H_2O_2 \quad (1)$$

The nature of the covalently bound cofactor in the CAOs had been the subject of speculation for several decades (*4*). In 1990, Janes *et al.* demonstrated unambiguously that the elusive cofactor was topa quinone (TPQ, Fig. 1A) (*5*), which was subsequently demonstrated to be derived from tyrosine (*6*). Although structurally very different from an earlier described quino-cofactor, pyrroloquinoline quinone (PQQ, Fig. 1B), the finding of TPQ in bovine serum amine oxidase extended the evidence for quino-cofactors from prokaryotes to mammalian systems. Shortly thereafter a third quino-structure derived from tryptophan, tryptophan tryptophylquinone (TTQ, Fig. 1C), was demonstrated in a bacterial amine dehydrogenase (*7*). From such findings, a family of "quinoproteins" can be defined to represent enzymes that use quinones as cofactors, where these cofactors may be either covalent species derived from amino acid side chains (TPQ and TTQ) or freely dissociable species (PQQ) (*8*). Thus far, only TPQ has been found to be ubiquitous, occurring in bacteria, yeast, plants, and mammals (*9*).

S. X. Wang, M. Mure, and J. P. Klinman are in the Departments of Chemistry and Molecular and Cell Biology, University of California, Berkeley, CA 94720, USA. K. F. Medzihradszky and A. L. Burlingame are in the Department of Pharmaceutical Chemistry and the Liver Center, University of California, San Francisco, CA 94143, USA. D. E. Brown and D. M. Dooley are in the Department of Chemistry and Biochemistry, Montana State University, Bozeman, MT 59717, USA. A. J. Smith is at the Beckman Center, Stanford University Medical Center, Stanford, CA 94305, USA. H. M. Kagan is in the Department of Biochemistry, Boston University School of Medicine, Boston, MA 02118, USA.

*Present address: Division of Structural Molecular Biology, Institute of Scientific and Industrial Research, Osaka University, Osaka 567, Japan.
†To whom correspondence should be addressed.

The relation of LO to the other CAOs has been the subject of considerable study and speculation. Both redox cycling assays (*10*) and enzyme inhibition patterns (*11*, *12*) indicate that LO contains a quinone-like structure at its active site. Resonance Raman studies of a COOH-terminal, cyanogen bromide cleavage product indicated spectral similarities to PQQ (*13*). In light of the finding of TPQ in a wide range of CAOs, the presence of TPQ in LO appeared more feasible. However, the large size differential between LO and other amine oxidases (*9*), as well as the fact that the TPQ consensus sequence (*14*) is absent in LO (*15*), raised the possibility of a different cofactor existing in LO. We have now isolated and characterized an active site, cofactor-containing peptide from bovine aorta LO. Investigation of this peptide by a combination of Edman sequencing, mass spectrometry, and resonance Raman spectroscopy indicates a type of quino-cofactor, previously undescribed, that is derived from the crosslinking of a modified Tyr to the ε-amino group of a lysyl side chain.

Protein isolation, proteolytic digestion, and characterization of peptides. LO was isolated from calf (2-week-old) aorta by a modification of a previously described procedure (*16*). A typical preparation of LO yielded about 5 mg (starting with about 500 g of aorta tissue). To minimize protein loss, we stopped purification after the stage where LO (32 kD) coeluted with a second protein (24 kD) from Sephacryl S-200 gel filtration. Further purification to eliminate this second protein resulted in partial loss of LO activity. The preparation of LO (referred to as two-banded material) was labeled with [^{14}C]phenylhydrazine to yield the expected chromophore (at about 450 nm) for a phenylhydrazone derivative of a quinone structure (*17*).

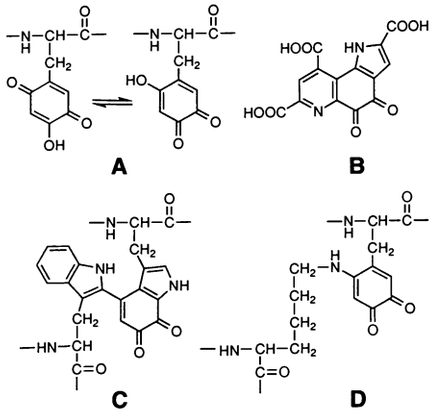

Fig. 1. Structures of the quinone cofactors: (**A**) topa quinone (TPQ), (**B**) pyrroloquinoline quinone (PQQ), (**C**) tryptophan tryptophylquinone (TTQ), and (**D**) lysine tyrosylquinone (LTQ).

Analysis of the ^{14}C-labeled protein by SDS–polyacrylamide gel electrophoresis (SDS-PAGE) showed almost exclusive incorporation of ^{14}C into the 32-kD LO band (Fig. 2). Because selection of active site–derived peptides from LO was dependent on screening for ^{14}C, we concluded that the unreactive 24-kD band would not contribute to subsequent procedures. Previous studies suggested that protein bands of 22 to 24 kD, copurifying with LO, are either degradation products of LO (*18*) or a contaminating matrix protein that elutes with LO in the course of purification (*19*).

The labeled protein was subjected to proteolytic digestion. Initially, a range of proteases and experimental conditions was examined. Thermolytic digestion of reduced and carboxyamidomethylated LO (or carboxymethylated LO in early procedures, such as that in Table 1) in the presence of 3 to 4 M urea was found to be the most acceptable procedure, giving a dominant [^{14}C]peptide peak under conditions of analytical high-performance liquid chromatography (HPLC) (*20*).

Ultraviolet-visible (UV-Vis) monitoring of the HPLC elution profile of a thermolytic digest of the [^{14}C]phenylhydrazine derivative of LO showed a large number of peptide peaks at 214 nm, together with a single dominant peak at 438 nm reflecting the phenylhydrazone (at 36 to 37 min) (*21*). In all instances, the ^{14}C radioactivity in peptide fractions was found to coincide with the 438-nm peaks. The peptide fraction eluting at 36 min was subjected to a second HPLC purification step before further analysis. The yield of this dominant 438-nm peak was 20 to 30 percent, estimated by comparing the radioactivity with the lyophilized peptide fraction with the

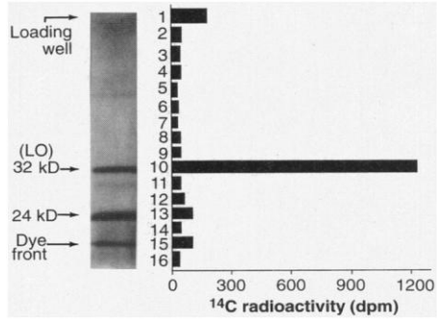

Fig. 2. Incorporation of ^{14}C-labeled phenylhydrazine in the two-banded (32-kD) LO protein. The desalted, labeled protein was separated by SDS-PAGE. (**Left**) The stained protein gel was cut into 16 slices according to the position of the protein bands (indicated by the numbers next to the gel). The gel slices were then dissolved in 1 to 5 ml of 2 percent periodic acid solution, and radioactivity in the solution was counted. (**Right**) The radioactivity in each gel slice.

total radioactivity in the proteolysis solution before HPLC purification. Integration of radioactivity in all fractions displaying 438-nm absorbance indicated close to 100 percent recovery of ^{14}C from the HPLC column.

The Edman sequencing result of a carboxymethylated thermolytic peptide isolated under the above conditions revealed two amino acids in early rounds of sequencing (Table 1). The recovery suggested the presence of two peptides. Comparison of the sequence determined (from bovine aorta) with the available cDNA-derived LO protein sequence (from rat aorta) (*15*) showed that both peptides (identified as peptides 1 and 2) were present in the protein (Table 1). Comparison of cDNA-derived sequences for LOs isolated from different sources indicates a high degree of conservation (*22*), with more than 93 percent identity among the 217 amino acids from the COOH-terminal region. In our sample, only single amino acids were detected in cycles 2, 4, and 6, and no amino acid was recovered at cycle 9 (Table 1). In the longer peptide (identified as peptide 1), the expected Ser at cycle 2 was indistinguishable from the background in the sequence analysis. This is not unusual when Ser occurs early in a sequence analysis. The blank at cycle 9 corresponds to a Tyr in the cDNA-derived sequence. Gly was expected in both sequences at cycle 4, and the anticipated Lys at cycle 6 at peptide 2 was missing. Two possibilities emerged; either an active site peptide with a crosslink between the Tyr of peptide 1 (at cycle 9) and the Lys of peptide 2 (at cycle 6) had been isolated from LO, or a mixture of unrelated peptides had been copurified. Because analysis of purified active site peptides isolated from different digestion pools showed the same pattern of two sequences, we favored the former explanation.

We next designed a strategy to reduce the size of the dominant thermolytic peptide, with the expectation that this would facilitate its separation from any contaminating peptide. Further digestion of the thermolytic peptide with Asp-N endoproteinase (*23*), a specific protease that cleaves to the NH_2-terminus of Asp residues, led to a fraction that ran as a single ^{14}C-labeled peak on reversed-phase HPLC. Sequencing of this fraction again indicated two amino acids in most cycles at about the same yield and a third peptide at a significantly lower recovery level (Table 2). Further purification of the subdigested peptide or peptides under a range of HPLC conditions yielded sequence data very similar to those given in Table 2.

As in the case of the Edman degradation of the thermolytic peptide (Table 1), only one amino acid was detected in cycle 3 at the expected level of recovery (Table 2). The anticipated Tyr^{349} (numbered after the cDNA-derived sequence) was not found in peptide 1. There is a lack of alignment between the isolated peptide sequence (from calf aorta) and cDNA-derived protein sequence (from rat aorta) in cycle 4, with the peptide sequence indicating Asn and the cDNA-derived protein sequence indicating Ala. We note that this position is not conserved among the cDNA-derived LO sequences determined from different species (*22*). A sudden drop in yield at the last round of sequencing is a common occurrence and may explain the low yield of both amino acids at cycle 6. For this reason, we could not demonstrate unambiguously that the low yield for Lys at position 6 of peptide 2 was because of its presence within a crosslinked structure. However, the fact that a thermolytic peptide precursor had been subdigested, and the resulting product repurified as a single peak by HPLC, made it highly unlikely that the material analyzed (Table 2) was a mixture of two peptides. We therefore concluded that the Asp-N–subdigested peptide was composed of a crosslink between the residue at position 3 in peptide 1 and position 6 in peptide 2. The low level of Lys at position 6 could arise either from breakdown of the proposed crosslinked species under the conditions of Edman sequencing (*24*) or from the presence of the third peptide at a much lower recovery level (Table 2).

Mass spectrometric analyses of the Asp-N–subdigested peptide. The cofactor-containing peptide from the thermolysin and Asp-N digest [sample 1, described in (*21*) and (*23*)] was further purified by microbore reversed-phase HPLC and the eluent directly introduced into an electrospray ionization mass spectrometer (LC-ESIMS analysis). The mass spectrum showed doubly and triply protonated ions at mass-to-charge ratios (m/z) of 720.9 (73%) and 480.9 (100%), respectively (*25*). These val-

Table 1. Edman sequencing of the thermolytic peptide.

Cycle	Thermolytic peptide		cDNA-derived* protein sequence	
	Amino acids† in each cycle		Peptide 1	Peptide 2
1	Multiple		Leu^{341}	Val^{309}
2		Ala	Ser	Ala
3	Pro	Glu	Pro	Glu
4	Gly		Gly	Gly
5	cmCys‡	His	Cys	His
6	Tyr		Tyr	Lys^{314}
7	Asp	Ala	Asp	Ala
8	Thr	Ser	Thr	Ser^{316}
9§			Tyr^{349}	
10	Asn		Ala	
11	Ala	Glu	Ala	
12	Asp		Asp	
13	Ile		Ile	
14	Asp		Asp	
15	(cmCys‡)		Cys	
16	(Gln)		Gln^{356}	

*The numbers are the residue numbers for the cDNA-derived protein sequence for rat LO (*15*). †The amino acids in each cycle are ordered for comparison with the cDNA-derived sequence so that they correspond to peptides 1 and 2, respectively. Thus, their appearance in each cycle (from left to right) is not necessarily related to yield. The yield of amino acids in cycles 2 to 16 ranged from 86 pmol to about 1 pmol, respectively. The amino acids that gave low signals are shown in parentheses. ‡cmCys represents carboxymethylated Cys residue. §A blank appeared at this cycle in Edman sequencing.

Table 2. Edman sequencing of the Asp-N subdigested peptide. A third peptide was detected at about 10 percent yields, relative to peptides 1 and 2. The sequence of this peptide—Leu, Ile, Phe, blank, Thr, (Met)—is not present in the cDNA sequence of rat LO.

Cycle	Peptide 1		Peptide 2	
	Amino acid	Yield (pmol)	Amino acid	Yield (pmol)
1	Asp	435	Val	397
2	Thr	167	Ala	323
3*			Glu	260
4	Asn	173	Gly	246
5	Ala	153	His	116
6	(Asp)	(20)	(Lys)	(10)

*Only Glu was observed at the expected recovery level in cycle 3.

Table 3. Molecular mass data of peptides after thermolysin and Asp-N treatment. Fractions absorbing at 438 nm, after thermolytic digestion, were pooled and subdigested with Asp-N. The resulting Asp-N digestion products were separated by HPLC before mass spectrometric analysis. The molecular mass was determined on a Micromass TofSpec SE matrix-assisted laser desorption ionization (MALDI) time-of-flight (TOF) mass spectrometer in reflectron mode, with α-cyano-4-hydroxycinnamic acid as the matrix. All active site peptides were studied by MALDI post source decay fragmentation.

Sample	MH^+	Change in basic structure*
3	1324.4	−Asp
4	1597.6	+Ala + Ser
6	1439.5	None
7	1482.5	−Asp + Ala + Ser

*The basic structure of the crosslinked peptide is shown underlined below (sample 1). The amino acids that are added to or subtracted from the basic structure are shown in bold.

Asp-Thr-(Tyr-derivative)-Asn-Ala-**Asp**

Val-Ala-Glu-Gly-His-(Lys-derivative)-**Ala-Ser**

ues were used to establish the chemical average (26) molecular mass as 1439.71 daltons. Subtraction of the residue weights of the known amino acid residues (two Asp, Thr, Asn, two Ala, Val, Glu, Gly, His) in the peptide, plus masses corresponding to two NH_2-terminal protons and two COOH-terminal hydroxyl groups, yielded a mass of 393.45 daltons as the residue weight for the unknown crosslinked cofactor structure labeled with phenylhydrazine.

To calculate the elemental composition of an ion, its mass must be measured to three or four decimal places. The accurate mass measurement was acquired on another peptide sample (sample 2) isolated from different thermolytic and Asp-N digests (27). The accurate mass value obtained for $[M+3H]^{3+}$ of sample 2 was 533.2356 daltons with a standard deviation of 0.0026, which establishes the monoisotopic (26) molecular mass of this peptide as 1596.6833 daltons. From the protein sequence and tandem mass spectra, sample 2 is an elongated version of peptide sample 1, possessing an Ala-Ser sequence at the COOH-terminus of the crosslinked Lys residue. Subtraction of the residue weights of the amino acid residues known to be present in this peptide, plus masses corresponding to two NH_2-terminal protons and two COOH-terminal hydroxyl groups, yielded a mass of 393.1830 daltons for the crosslinked residue (or 288.1377 daltons after further subtraction of the phenylhydrazine label). Computer calculation gives a composition of $C_{21}H_{23}N_5O_3$ ($C_{15}H_{18}N_3O_3$ without the phenylhydrazine label), which shows a −10.0 parts per million deviation from the measured mass value.

A reasonable structure for the phenylhydrazine derivative of the cofactor is shown below (as two possible tautomers).

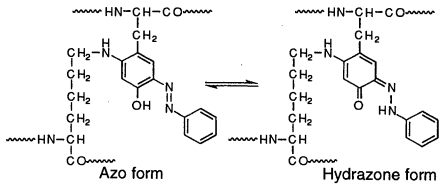

The cofactor itself is proposed to have the structure shown in Fig. 1D. This is consistent with the strong evidence for a quinone-like structure in LO (10, 12, 13, 28) and with the finding that the cofactor comprises a crosslink between a Tyr derivative and a Lys residue. Such a cofactor structure could arise from an initial hydroxylation of Tyr to form 3,4-dihydroxyphenylalanine (dopa), followed by the oxidation of dopa to dopa quinone, and subsequent nucleophilic attack by the ε-amino group of a Lys side chain to generate an aminoquinol (Scheme 1, path A).

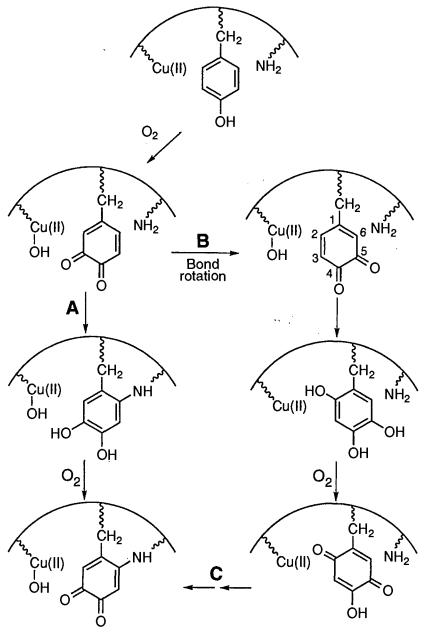

Scheme 1. Proposed mechanism for the generation of lysine tyrosylquinone.

In the course of these studies, HPLC sample fractions containing active site peptides derived from thermolytic digests were pooled, subjected to further digestion with Asp-N, and subsequently analyzed by mass, spectrometry. The monoisotopic MH^+ ions observed in these experiments (for samples 3, 4, 6, and 7) are shown in Table 3. The finding of cleavage site heterogeneity is consistent with the known nonspecific nature of thermolysin, whereby the enzyme could cleave either between the modified Lys and Ala or between Ser and Phe in peptide 2. Because endoproteinase Asp-N is a poor catalyst as an exoproteinase (29), it is not surprising to see the sequence variations (with the Asp residue cleaved or retained) at the COOH-termini in the peptides purified from different digestion pools.

One of these peptides (sample 4) was subjected to high-energy collision-induced dissociation (CID) analysis (Fig. 3). The monoisotopic ^{12}C isobar of MH^+ (at m/z of 1597.6) was selected as the precursor ion. Immonium ions (H_2N^+=CH–R) at m/z of 72 and 110 show the presence of unmodified Val and His residues, respectively. Ions at m/z of 167 and 367 correspond to internal immonium fragments GH−28 and AEGH−28 [−28 daltons indicates loss of the carbonyl (CO)], respectively. The sequence ion at m/z of 494 (b_5) suggests the presence of the NH_2-terminal VAEGH sequence without modification, and the fragment at m/z of 466 (a_5) is present because of CO loss from the b_5 ion. Other b-type fragments detected at m/z of 1492 and 1421 indicate the loss of the COOH-terminal Ser and Ala-Ser, respectively. Fragment ions

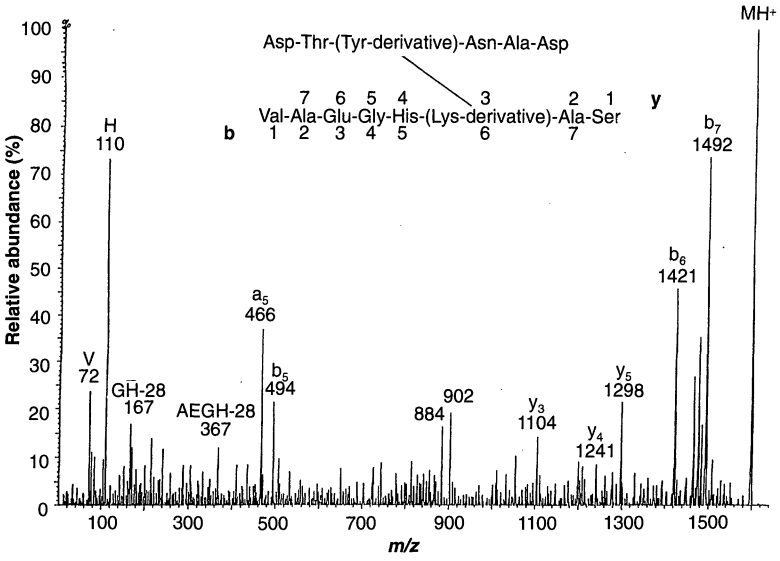

Fig. 3. MALDI–high-energy CID mass spectrum of a phenylhydrazine-derivatized active site peptide (sample 4 in Table 3). This experiment was done on a Micromass AutoSpec SE orthogonal acceleration–TOF tandem mass spectrometer. Fragmentation occurred for the most part along the backbone of peptide 2. Fragments are labeled as proposed (42). When the peptide bond is cleaved, a y-type sequence ion is formed with charge retention at the COOH-terminus (such as y_3, y_4, and y_5); if the charge is retained at the NH_2-terminus, a b-type sequence ion is formed (such as b_5, b_6, and b_7). A loss of carbonyl from a b-ion leads to the formation of an a-ion (such as a_5). Abbreviations for the amino acid residues are as follows: A, Ala; C, Cys; D, Asp; E, Glu; F, Phe; G, Gly; H, His; I, Ile; K, Lys; L, Leu; M, Met; N, Asn; P, Pro; Q, Gln; R, Arg; S, Ser; T, Thr; V, Val; W, Trp; and Y, Tyr.

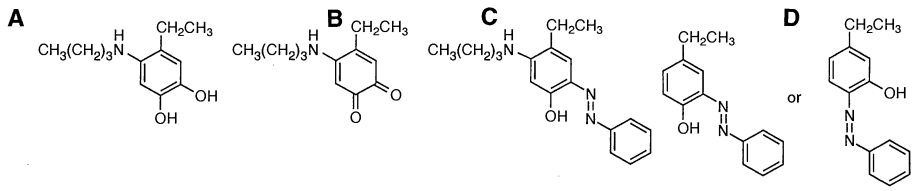

Fig. 4. Structure of the synthetic model compounds. The reduced form of LTQ model (**A**), the oxidized quinone form (**B**), and the phenylhydrazine derivative (**C**). (**D**) The phenylhydrazine derivative of ethyldopa quinone.

at m/z of 1298, 1241, and 1104 are y-ions, indicating the loss of VAE, VAEG, and VAEGH sequences. The fragment ion at m/z of 902 is a result of cleavages between the α and β carbon of the modified Tyr residue (−590 daltons) and a cleavage between the aromatic ring and the phenylhydrazine label (−105 daltons), with charge retention on the NH_2-terminal fragment. The ion at m/z of 884 seems to be formed by cleavages between the amino group and the α carbon, and between the α carbon and the CO group of the Lys residue with charge retention on the crosslinked residue or peptide 1. This CID spectrum, together with similar results on other crosslinked peptides, provides independent evidence for the proposed crosslinked cofactor structure and the crosslinking site in the protein.

Synthesis and characterization of a model for the LO cofactor. In order to confirm the structure for the LO cofactor, it was essential to have a synthetic model compound resembling the proposed enzymic structure. Model compounds were designed and synthesized (*30*). Three forms of one such structure are shown as reduced quinol (Fig. 4A), oxidized quinone (Fig. 4B), and phenylhydrazine derivative (Fig. 4C).

One of the characteristics of the UV-Vis absorption spectrum of LO is an absorption maximum wavelength (λ_{max}) at about 510 nm (Fig. 5), which is 20 to 30 nm red-shifted relative to TPQ-containing CAOs and models thereof (with typical λ_{max} values of about 480 nm). As shown in Fig. 5, the oxidized form of the LO model compound (Fig. 4B) displays a λ_{max} of 504 nm (or 506 nm in urea buffer). Almost exact correspondence was observed for the absorbance of the phenylhydrazine-labeled LO protein and the phenylhydrazine derivative of the lysine tyrosylquinone (LTQ) model compound (Fig. 4C), with values for λ_{max} of 454 and 452 nm, respectively (*31*).

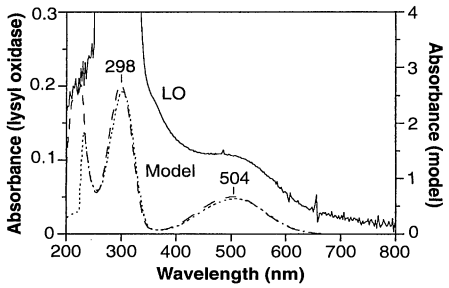

Fig. 5. Comparison of UV-Vis absorption properties of native LO to the model compound (Fig. 4B). The spectrum of LO was taken in 16 mM potassium phosphate containing 6 M urea, pH 7.8 (solid line). The spectrum of the model was taken either in 16 mM potassium phosphate, pH 7.8 (broken line), or in 16 mM potassium phosphate containing 6 M urea, pH 7.8 (dotted line).

More detailed comparisons of spectra were performed with resonance Raman spectrometry on the isolated active site peptide and the model compound. Because the isolated active site peptide contained the cofactor as its phenylhydrazine derivative, these studies were restricted to the phenylhydrazine derivative of the model compound. Although the latter compound showed only limited solubility in water, both the active site peptide and the model compound dissolved readily in 0.5 percent trifluoroacetic acid and 2 percent acetonitrile (CH_3CN). Under these conditions, spectra for both samples were almost superimposable (Fig. 6, A and B) and distinct from a TPQ model compound under the same conditions (Fig. 6C). It is generally recognized that resonance Raman spectroscopy can provide spectral information that is sensitive to conformational and environmental factors. Although structurally related compounds may display features in common, superimposable spectra indicate the same chromophore in identical environments. The *n*-butyl and ethyl side chains of the model compound appear to provide an excellent match for the LO active site–derived peptide, under the denaturing conditions of low pH and acetonitrile.

Mutagenesis studies on LO. The above-documented sequencing, mass spectrometric analyses, and spectral characterizations indicate structure D in Fig. 1 as the active site cofactor of LO. Sequence alignment of the isolated peptide to the cDNA sequence identified the crosslinking Lys and Tyr residues as Lys^{314} and Tyr^{349}. When the eukaryotic expression system for rat aorta LO is used, low amounts of protein suitable for activity assays are produced (*32*). Site-directed mutagenesis studies were undertaken and the results are summarized in Table 4. The Y349F mutant (in which the Tyr residue at position 349 is mutated to Phe) was completely inactive, whereas mutation of a different Tyr residue (Y328F, as a control) led to an enzyme with full activity. The K314A mutant was also inactive. The activity of the Y349F-K314A double mutant, as compared

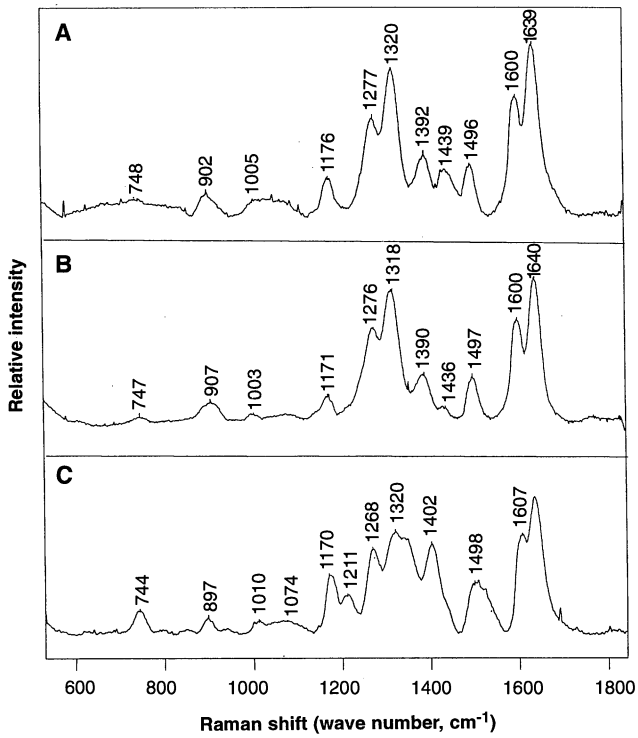

Fig. 6. Comparison of resonance Raman spectra for the labeled peptide from LO to the corresponding synthetic LTQ and TPQ model compounds. The excitation wavelength is 457.9 nm, with power of 40 mW. Shown here are the spectra for (**A**) the labeled LO active site peptide, (**B**) the phenylhydrazine derivative of LTQ model (Fig. 4C), and (**C**) the phenylhydrazine derivative of topa hydantoin quinone.

with the wild-type enzyme, was within the background limits of the tritium release assay method. These results support Lys^{314} and Tyr^{349} as the sites of cofactor crosslinking.

Relation of the LO cofactor to other cofactors in quinoenzymes. Our studies present evidence for a variant quinone cofactor in a mammalian system. To compare the redox properties of this previously unknown cofactor (now designated LTQ) with TPQ, we undertook cyclic voltammetric studies. The LTQ model compound has a midpoint potential (E_m) of −181 mV at pH 6.7, identical to a *t*-butyl-TPQ model compound and similar to PQQ and the topa hydantoin quinone model compound (Table 5). These data suggest that the different biological roles for PQQ, TPQ, and LTQ lie in their reductive half-reactions and not in the regeneration of oxidized cofactor from their quinol forms.

Of great interest is the fact that LTQ is derived from Tyr, analogous to the origin of TPQ, suggesting that the biogenesis of LTQ and TPQ may be similar. Studies from both this laboratory (*33*, *34*) and that of Tanizawa and co-workers (*35*) have shown TPQ to arise by a self-processing mechanism that involves the protein-bound copper. A possible mechanism for the biogenesis of LTQ is presented in Scheme 1. By analogy with TPQ, the conversion of peptidyl Tyr to dopa is proposed to occur by ring hydroxylation to yield dopa quinone. In the case of TPQ (Scheme 1B), a bond rotation about the β carbon (*36*) would place the electrophilic carbon (C-2) of dopa quinone in proximity to a copper-bound hydroxide ion (or water), which is positioned for nucleophilic attack at the C-2 position (*6*, *34*). Although not indicated in Scheme 1, a similar bond rotation may occur in LTQ biogenesis, depending on the geometric orientation of Lys^{314} within the active site. Scheme 1C shows an alternative pathway for LTQ biogenesis, in which TPQ is formed first, followed by attack of a lysyl side chain at the C-2 carbonyl of TPQ to generate LTQ. Model studies of TPQ analogs in their ionized anionic form have indicated that amines react exclusively at the C-5 carbonyl (*37*), suggesting that Scheme 1C would only be feasible if a TPQ precursor to LTQ were protonated at C-4. Given the low pK_a (about 3, where K_a is the acid dissociation constant) determined for TPQ in bovine serum amine oxidase (*37*), we consider this highly unlikely, strongly favoring pathway A in Scheme 1 for LTQ biogenesis.

We have considered the possibility that the mature cofactor in LO was dopa quinone (the postulated biogenetic intermediate), which had undergone fortuitous crosslinking with a Lys in the course of active site peptide isolation. To address this possibility, we reacted 4-ethyl-1,2-benzoquinone with phenylhydrazine to obtain a derivative (*38*). The isolated phenylhydrazine derivative was found to have a λ_{max} of about 330 nm, which is distinct from the phenylhydrazine adduct of both LO protein and the LTQ model compound (with λ_{max} values of 454 and 452 nm, respectively). ^1H nuclear magnetic resonance (NMR) of the isolated product showed that the hydrazine derivatives (isolated as a mixture of two isomers) were in an azo form with the cofactor ring reduced (see Fig. 4D for structures). Consistent with an anticipated unreactivity of such an azo compound toward nucleophilic attack by amines, no reaction was observed after overnight incubation of compound D (Fig. 4) with a 1000-fold excess of propylamine (*38*). A spurious side reaction in the course of cofactor isolation may, therefore, be ruled out as the source of the observed structure.

Our findings raise a number of provocative questions regarding quinoproteins and LO. The proposed biogenetic pathways for TPQ (*6*, *34*) and LTQ (Scheme 1) invoke a common *o*-quino intermediate that reacts with either water or Lys and suggest the possibility of other, naturally occurring TPQ analogs. These TPQ analogs may differ with regard to the nature of the substituent at the C-2 position of the cofactor and arise by reaction of other nucleophilic side chains (such as Asp or Glu, Ser, and Cys) with a dopa quinone precursor. It is appropriate to question whether LTQ is restricted to LO or whether it occurs in other enzymes as well. Among the CAOs, the membrane-associated semicarbazide-sensitive amine oxidases remain to be characterized with regard to overall protein sequence and cofactor identification. Finally, it has been found that *rrg*, a putative tumor suppressor of *ras* expression, encodes LO (*39*). The downregulation of LO expression in transformation and the induction of LO in interferon-mediated reversion of transformed cells suggests that this enzyme has a role in tumor suppression. It is still not clear whether the *rrg* gene product is catalytically active, and in particular, whether LTQ biogenesis and LO catalysis participate in the reversion of the tumorigenic state (*40*).

Table 4. Mutagenesis studies on LO. WT corresponds to wild-type LO, in which the enzyme was secreted into the medium of Chinese hamster ovary (CHO) cells transfected with a full-length LO construct (*32*). DHFR(−) corresponds to CHO cells transfected with the dihydrofolate reductase selection plasmid only, which lacks the LO cDNA insert. Enzyme activity was determined as described (*41*) and represents ^3H released from a 2-hour incubation. Typically, for an assay of about 700 cpm ^3H released in 2 hours, the background counts can range from 70 to 100 cpm (up to 15 percent). Immunoblot analysis with rabbit antibodies to LO as the probe indicated that the concentrations of mutant proteins ranged from about 50 to 100 percent of the wild-type LO.

Protein assayed	Activity	
	cpm	Percent of WT
WT	688 ± 25	100 ± 4
Y349F	6 ± 1	0.9 ± 0.2
Y328F	660 ± 30	96 ± 4
K314A	0 ± 17	0 ± 3
Y349F-K314A	39 ± 2	6 ± 0.3
DHFR(−)	9 ± 2	1.3 ± 0.3

Table 5. Midpoint potentials (E_m) for different quinone cofactors. Cyclic voltammetry was carried out at pH 6.7 with a three-electrode system consisting of a gold working electrode (electrode area of 0.02 cm^2), a coiled platinum counter electrode, and a saturated calomel electrode (SCE) as the reference.

Model compounds	E_m versus SCE (mV)
PQQ	−155
Topa hydantoin quinone	−149
t-Butyl-TPQ	−181
LO model quinone	−181

REFERENCES AND NOTES

1. S. R. Pinnell and G. R. Martin, *Proc. Natl. Acad. Sci. U.S.A.* **61**, 708 (1968).
2. H. M. Kagan, in *Biology of Extracellular Matrix: A Series Regulation of Matrix Accumulation* (Academic Press, Orlando, FL, 1986), vol. 1; D. R. Eyre, M. A. Paz, P. M. Gallop, *Annu. Rev. Biochem.* **53**, 717 (1984); L. B. Sandberg, N. T. Soskel, J. G. Leslie, *N. Engl. J. Med.* **304**, 566 (1981).
3. K. I. Kivirikko and H. Kuivaniemi, in *Connective Tissue Disease*, J. Uitto and A. J. Peredja, Eds. (Dekker, New York, 1987); D. W. Rowe, E. B. McGoodwin, G. R. Martin, D. Grahn, *J. Biol. Chem.* **252**, 939 (1977); P. H. Byers *et al.*, *N. Engl. J. Med.* **303**, 61 (1980); H. Kuivaniemi, L. Peltonen, A. Palotie, I. Kaitila, K. I. Kivirikko, *J. Clin. Invest.* **69**, 730 (1982); H. Kuivaniemi, L. Peltonen, K. I. Kivirikko, *Am. J. Hum. Genet.* **37**, 798 (1985); P. M. Royce, J. Camakaris, D. M. Danks, *Biochem. J.* **192**, 579 (1980).
4. F. Buffoni, *Pharmacol. Rev.* **18**, 1163 (1966); K. T. Yasunobu, H. Ishizaki, N. Minamiura, *Mol. Cell. Biochem.* **13**, 3 (1976); T. A. Bird and C. I. Levene, *Biochem. Biophys. Res. Commun.* **108**, 1172 (1982); P. F. Knowles and K. D. S. Yadav, in *Copper Proteins and Copper Enzymes*, R. Lontie, Ed. (CRC Press, Boca Raton, FL, 1984), vol. 2, pp. 103–129; G. A. Hamilton, in *Copper Proteins*, T. G. Spiro, Ed. (Wiley, New York, 1981); R. H. Suva and R. H. Abeles, *Biochemistry* **17**, 3538 (1978); R. A. van der Meer, A. C. Mulder, J. A. Jongejan, J. A. Duine, *FEBS Lett.* **254**, 99 (1989); P. F. Knowles *et al.*, *Biochem. J.* **241**, 603 (1987); R. S. Moog, M. A. McGuirl, C. E. Cote, D. M. Dooley, *Proc. Natl. Acad. Sci. U.S.A.* **83**, 8435 (1986); R. A. van der Meer and J. A. Duine, *Biochem. J.* **239**, 789 (1986).
5. S. M. Janes *et al.*, *Science* **248**, 981 (1990).
6. D. Mu *et al.*, *J. Biol. Chem.* **267**, 7979 (1992).
7. W. S. McIntire, D. E. Wemmer, A. Christoserdov, M. E. Lidstrom, *Science* **252**, 817 (1991).
8. S. A. Salisbury, H. S. Forrest, W. B. T. Cruse, O. Kennard, *Nature* **280**, 843 (1979).
9. J. P. Klinman and D. Mu, *Annu. Rev. Biochem.* **63**, 299 (1994).
10. M. A. Paz, R. Fluckiger, A. Boak, H. M. Kagan, P. M. Gallop, *J. Biol. Chem.* **266**, 689 (1991).
11. F. Buffoni, G. Ignesti, M. Lodovici, *Ital. J. Biochem.*

30, 179 (1981).
12. S. N. Gacheru, P. C. Trackman, S. D. Calaman, F. T. Greenaway, H. M. Kagan, *J. Biol. Chem.* **264**, 12963 (1989).
13. P. R. Williamson, R. S. Moog, D. M. Dooley, H. M. Kagan, *ibid.* **261**, 16302 (1986).
14. S. M. Janes *et al.*, *Biochemistry* **31**, 12147 (1992).
15. P. C. Trackman *et al.*, *ibid.* **29**, 4863 (1990).
16. H. M. Kagan, K. A. Sullivan, T. A. Olsson, A. L. Cronlund, *Biochem. J.* **177**, 203 (1979); M. A. Williams and H. M. Kagan, *Anal. Biochem.* **149**, 430 (1985).
17. The enzyme showed two bands on SDS-PAGE; the specific activity was 0.019 U/mg when assayed at pH 7.2 with benzylamine as the substrate. LO (6.34 mg) was dissolved in 16 mM potassium phosphate (pH 8.0) containing 3.43 M urea and reacted with 240 nmol of [^{14}C]phenylhydrazine hydrochloride (universally labeled 5550 dpm/nmol) for about 30 minutes. A chromophore was formed at the wavelength (λ_{max}) of 454 nm. Typically, the stoichiometry of labeling is about 40 to 50 percent after correction for the presence of the second band in the LO preparation.
18. K. A. Sullivan and H. M. Kagan, *J. Biol. Chem.* **257**, 13520 (1982); H. Kuivaniemi, E. Savolainen, K. Kivirikko, *ibid.* **259**, 6996 (1984); P. D. Burbelo, A. Monckeberg, C. O. Chichester, *Collagen Relat. Res.* **6**, 153 (1986).
19. A. D. Cronshaw *et al.*, *Matrix* **13**, 255 (1993).
20. *The [^{14}C]phenylhydrazine-labeled protein (see Fig. 2) was prepared in 6 M guanidine hydrochloride,* reduced by dithiothreitol, and subsequently alkylated with iodoacetamide (*29*). After desalting, the reduced and carboxyamidomethylated protein sample was prepared in 100 mM NH_4HCO_3 (pH 8.0) containing 2 M urea at 37°C, with shaking. Proteolytic digestion was initiated by the addition of thermolysin to 4 percent (w/w). A second portion of the protease was added after 24 hours. The digestion was stopped after 49 hours by cooling the solution at −70°C.
21. Thermolytically digested enzyme was injected onto a Dynamax reversed-phase C18 column, equilibrated with solvent A [0.11 percent trifluoroacetic acid (TFA), 5 percent CH_3CN, H_2O] on a Shimadzu HPLC system. Peptides were eluted with solvent B (0.1 percent TFA, 80 percent CH_3CN, H_2O) with a linear gradient of 20 to 30 percent solvent B over 65 minutes at a flow rate of 1 ml per minute. Elution of peptides was monitored at 214 and 438 nm. The yield was 22 percent for the 36-minute peak based on radioactivity relative to that contained in the digestion solution.
22. Y. Kim, C. D. Boyd, K. Csiszar, *J. Biol. Chem.* **270**, 7176 (1995).
23. The predominant peak at 438 nm was lyophilized and redissolved in 50 mM sodium phosphate (pH 8.0). Subdigestion was initiated by the addition of Asp-N endoproteinase to a final concentration of 2.5 percent (w/w). The digestion mixture was incubated at 37°C with gentle shaking for 19 hours and later stored at −70°C. Peptides resulting from the digest were again separated on HPLC by a modification of a previously described procedure (*5*). A Vydac reversed-phase C18 column was used, and peptide elution was monitored at 220 and 438 nm. The single peak containing the active site peptide was collected, lyophilized, and subsequently used for sequencing, mass spectrometry, and resonance Raman studies. Overall yield for this single peak was about 26 percent relative to total peptides in the Asp-N digestion reaction. This corresponded to about 1.2 nmol of the active site peptide.
24. P. Edman and G. Begg, *Eur. J. Biochem.* **1**, 80 (1967).
25. Electrospray mass spectrum of the phenylhydrazine-derivatized LO active site peptide (sample 1) referred to as "basic structure" was acquired in an LC-ESIMS experiment with a Micromass BioQ quadrupole *mass spectrometer equipped with an electrospray source. The mass spectrometer was scanned in* noncontinuum mode over a range of *m/z* as 350 to 2000 at 5 s per scan.
26. S. A. Carr and A. L. Burlingame, in *Mass Spectrometry in the Biological Sciences*, A. L. Burlingame and S. A. Carr, Eds. (Humana Press, Totowa, NJ, 1996), appendix XI, p. 546.
27. The accurate mass measurement was performed by Micromass AutoSpec SE spectrometry with electrospray ionization on the triply charged ion of a cofactor-containing peptide (sample 2) with doubly charged ions of bradykinin (*m/z* of 530.7885) and ceramicidin (*m/z* of 571.3608) as calibration standards.
28. P. R. Williamson, J. M. Kittler, J. W. Thanassi, H. M. Kagan, *Biochem. J.* **235**, 597 (1986).
29. G. Allen, in *Sequencing of Proteins and Peptides* (Elsevier, New York, ed. 2, 1989), p. 58.
30. S. X. Wang, M. Mure, J. P. Klinman, in preparation.
31. The UV conditions were as follows: The phenylhydrazine derivative of LO protein was in 16 mM potassium phosphate (pH 7.8) containing 3.43 M urea; the phenylhydrazine derivative of LO model compound was in 100 mM potassium phosphate (pH 7.7) containing 3 M urea (*30*).
32. H. M. Kagan *et al.*, *J. Cell. Biochem.* **59**, 329 (1995).
33. D. Cai and J. P. Klinman, *J. Biol. Chem.* **269**, 32039 (1994).
34. ———, *Biochemistry* **33**, 7647 (1994).
35. R. Matsuzaki, T. Fukui, H. Sato, Y. Ozaki, K. Tanizawa, *FEBS Lett.* **351**, 360 (1994); Y.-H. Choi *et al.*, *J. Biol. Chem.* **270**, 4712 (1995).
36. Ring flipping of TPQ has been confirmed by the crystal structure of the TPQ-containing amine oxidase from *Escherichia coli* [M. R. Parsons *et al.*, *Structure* **3**, 1171 (1995)].
37. M. Mure and J. P. Klinman, *J. Am. Chem. Soc.* **115**, 7117 (1991); *ibid.* **117**, 8707 (1995).
38. 4-Ethyl-1,2-benzoquinone was prepared by oxidation of 4-ethylcatechol with Ag_2O in ether. The isolated quinone compound was then reacted with phenylhydrazine hydrochloride in dry methanol to make the phenylhydrazine derivatives, which were confirmed by ^{1}H NMR to be in the azo forms (Fig. 4D). The azo adducts at a concentration of 8.50×10^{-5} M and *n*-propylamine at a final concentration of 8.51×10^{-2} M were incubated overnight in anhydrous acetonitrile. The reaction process was monitored by taking UV-Vis spectra at various reaction times. The final reaction mixture was examined by analytical HPLC.
39. K. Kenyon *et al.*, *Science* **253**, 802 (1991).
40. H. M. Kagan and P. C. Trackman, in *Principles and Applications of Quinoproteins*, V. L. Davidson, Ed. (Dekker, New York, 1993), pp. 173–189.
41. D. Bedell-Hogan, P. Trackman, W. Abrams, J. Rosenbloom, H. M. Kagan, *J. Biol. Chem.* **268**, 10345 (1993).
42. K. Biemann, *Methods Enzymol.* **193**, 886 (1990).
43. Supported by NIH research grants GM39296 (J.P.K.), and GM27659 (D.M.D.), National Center for Research Resources Biomedical Research Technology Program grants P41 RR01614 (A.L.B.), and R37 AR 18880 and HL 13262 (H.M.K.), and supported by the NSF Biological Instrumentation Program grant DIR 8700766 (A.L.B.).

27 March 1996; accepted 16 July 1996